Available online at www.sciencedirect.com
SCIENCE DIRECT®
International Journal of Pharmaceutics 292 (2005) 95–117
international journal of pharmaceutics
www.elsevier.com/locate/ijpharm

Dispersion of microemulsion drops in HEMA hydrogel: a potential ophthalmic drug delivery vehicle

Derya Gulsen, Anuj Chauhan*

Chemical Engineering Department, University of Florida, Room 237, CHE PO Box 116005, Gainesville, FL 32611-6005, USA

Received 5 December 2003; received in revised form 24 November 2004; accepted 24 November 2004
Available online 22 January 2005

Abstract

Approximately 90% of all ophthalmic drug formulations are now applied as eye-drops. While eye-drops are convenient and well accepted by patients, about 95% of the drug contained in the drops is lost due to absorption through the conjunctiva or through the tear drainage. A major fraction of the drug eventually enters the blood stream and may cause side effects. The drug loss and the side effects can be minimized by using disposable soft contact lenses for ophthalmic drug delivery. The essential idea is to encapsulate the ophthalmic drug formulations in nanoparticles, and disperse these drug-laden particles in the lens material. Upon insertion into the eye, the lens will slowly release the drug into the pre lens (the film between the air and the lens) and the post-lens (the film between the cornea and the lens) tear films, and thus provide drug delivery for extended periods of time. This paper focuses on dispersing stabilized microemulsion drops in poly-2-hydroxyethyl methacrylate (p-HEMA) hydrogels. The results of this study show that the p-HEMA gels loaded with a microemulsion that is stabilized with a silica shell are transparent and that these gels release drugs for a period of over 8 days. Contact lenses made of microemulsion-laden gels are expected to deliver drugs at therapeutic levels for a few days. The delivery rates can be tailored by controlling the particle and the drug loading. It may be possible to use this system for both therapeutic drug delivery to eyes and the provision of lubricants to alleviate eye problems prevalent in extended lens wear.

Keywords: Microemulsions; Ophthalmic drug delivery; Contact lenses; Hydrogel; HEMA

1. Introduction

The topical delivery of drugs by eye-drops currently accounts for about 90% of all ophthalmic formulations. This method of drug delivery is very inefficient and in some instances leads to serious side effects (Bourlais et al., 1998). Only about 5% of the drug applied as drops penetrates through the cornea to reach the intraocular

* Corresponding author. Tel.: +1 352 392 2592; fax: +1 352 392 9513.
E-mail addresses: dgulsen@ufl.edu (D. Gulsen), chauhan@che.ufl.edu (A. Chauhan).

0378-5173/$ – see front matter © 2004 Elsevier B.V. All rights reserved.
doi:10.1016/j.ijpharm.2004.11.033

tissue, while the rest is lost due to tear drainage (Lang, 1995). Upon instillation, the drug mixes with the fluid present in the tear film and has a short residence time of approximately 2 min in the film. About 5% of the drug gets absorbed into the cornea and the remaining either gets absorbed in the conjunctiva or flows through the upper and the lower canaliculi into the lacrimal sac (Lang, 1995). The drug containing tear fluid is carried from the lacrimal sac into the nasolacrimal duct. The nasolacrimal duct empties into the nasal cavity, where the drug gets absorbed into the bloodstream. This absorption leads to drug wastage, and more importantly, the presence of certain drugs in the bloodstream leads to undesirable side effects. For example, beta-blockers such as timolol (Timoptic®) that are used in the treatment of wide-angle glaucoma have also a deleterious effect on the heart. Furthermore, the application of ophthalmic drugs as drops results in a rapid variation in the drug delivery rates to the cornea and this limits the efficacy of the therapeutic systems (Segal, 1991). Thus, there is a need for new ophthalmic drug delivery systems that increase the residence time of the drug in the eye, thereby reducing wastage and minimizing side effects.

To reduce the drug loss and the systemic side effects, and improve the drug efficacy, we propose to develop disposable soft contact lenses as a new vehicle for ophthalmic drug delivery. The essential idea is to encapsulate the ophthalmic drug formulations in nanoparticles and disperse these drug-laden particles in the contact lens matrix (Fig. 1). If the nanoparticle size and loading are sufficiently low, the particle-loaded lenses are transparent. This project focuses on soft hydrogel lenses that are made of poly 2-hydroxyethyl methacrylate (HEMA). The p-HEMA hydrogel matrix can be synthesized by bulk or solution free radical polymerization of the HEMA monomers in the presence of a cross-linker such as ethylene glycol-di-methacrylate (EGDMA) (Mandell, 1974). The addition of drug-laden particles in the polymerizing medium results in the formation of a particle-dispersion in the hydrogel matrix. If contact lenses made of this material are placed on the eye, the drug is expected to diffuse from the particles, travel through the lens matrix, and enter the post-lens tear film (POLTF), i.e., the thin tear film trapped in between the cornea and the lens. In the presence of a lens, drug molecules will have a residence time of about 30 min in the post-lens tear film,

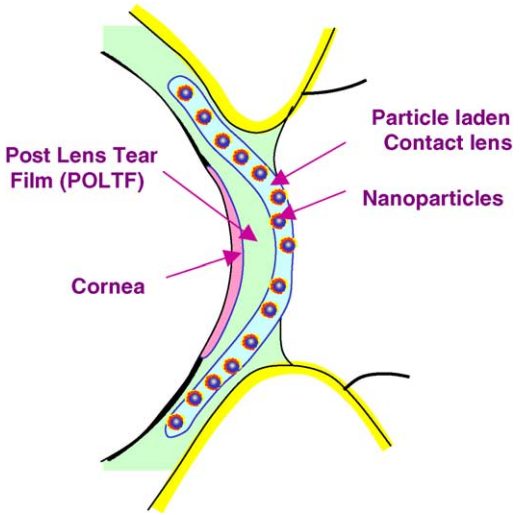

Fig. 1. Schematic illustration of the particle-laden lens inserted in the eye.

compared to about 2 min in the case of topical application as drops (Bourlais et al., 1998; Creech et al., 2001; Mc Namara et al., 1999). The longer residence time will result in a higher drug flux through the cornea and reduce the drug inflow into the nasolacrimal sac, thus reducing the drug absorption into the blood stream. In addition, due to the slow diffusion of the drug molecules through the particles and the lens matrix, drug-laden contact lenses can provide continuous drug release for extended periods of time.

A number of researchers have attempted to use contact lenses for ophthalmic drug delivery; however, all their efforts focused on soaking the lenses in a drug solution followed by insertion into the eye. While soaked contact lenses are perhaps more efficient at delivering medications than drops, they still suffer from some limitations. The maximum drug loading is limited by the solubility of the drugs in the gel matrix. Also the only resistance to drug transport is diffusion through the gel matrix, and thus, drugs can only be delivered for a limited period of time. One of the recent studies on the use of contact lenses for ophthalmic drug delivery focused on soaking the lens in eye-drop solutions for 1 h followed by lens insertion in the eye (Hehl et al., 1999). Five different drugs were studied and it was concluded that the amount of drug released by the lenses is considerably lower or of the same order of magnitude as the drug released by eye-drops.

In another study, researchers developed a compound contact lens with a hollow cavity by bonding together two separate pieces of lens material (Nakada and Sugiyama, 1998). The compound lens was soaked in the drug solution. The lens imbibed the drug solution and slowly released it upon insertion in the eyes. The compound lens suffers from the same limitations as the drug-soaked lens because the concentration of the drug in the cavity is the same as the concentration of the drug in the drops, and thus, such a lens can supply the drug for a limited amount of time. Furthermore, the presence of two separate sheets of lens material leads to smaller oxygen and carbon dioxide permeabilities, a situation that can cause an edema in the corneal tissue. The other studies and patents listed below suffer from the same limitations because they are also based on soaking of contact lenses or similar devices in drug solutions followed by insertion into the eye (Hillman, 1974; Ramer and Gasset, 1974; Montague and Watkins, 1975; Hillman et al., 1975; Giambattista et al., 1976; Marmion and Yardakul, 1977; Arthur et al., 1983; Wilson and Shields, 1989; Fristrom, 1996; Schultz and Mint, 2000; Rosenwald, 1981; Schultz et al., 1995).

A number of researchers have trapped proteins, cells, and drugs in hydrogel matrices by polymerizing the monomers that comprise the hydrogel in the presence of the species that needs to be entrapped (Elisseeff et al., 2000; Ward and Peppas, 2001; Scott and Peppas, 1999; Podual et al., 2000; Colombo et al., 1999; Ende and Peppas, 1997). Thus, another possible method to trap a drug in contact lenses is by dissolving the drug molecules directly in the polymerization mixture. However, this method is not very useful for hydrophobic drugs because of their limited solubility in the HEMA polymerizing mixture. Also, if drugs are simply dispersed in the lenses, they diffuse out of the gel in time that scales as h^2/D, where h is the gel thickness and D the diffusion coefficient of the drug in the gel, and since D and h are fixed by contact lens designers, one has no separate control over the drug release time scales. Another potential disadvantage of directly dissolving the drug molecules in the polymerization mixture is the possibility that drug molecules may become involved in the polymerization reaction and lose their functionality. These disadvantages can be overcome by providing a capsule that will entrap the drug and thus prevent interaction of the drug molecules with the polymerization mixture. Also, one will be able to dissolve more quantities of a drug and release it for longer periods of time by choosing appropriate nanoparticles.

Recently, Graziacascone et al. (2002) published a study on encapsulating lipophilic drugs inside nanoparticles and entrapping the particles in hydrogels. They used PVA hydrogels as hydrophilic matrices for the release of lipophilic drugs loaded in PLGA particles. They compared the drug release rates from hydrogels loaded with the particles with the delivery rates directly from the PLGA particles and found comparable results, which implies that the particles controlled the drug release rates. This current paper deals with the incorporation of drug-laden nanoparticles in a p-HEMA contact lens matrix in a manner such that the particle-laden gels are transparent and can release drugs at therapeutic rates.

This paper specifically focuses on encapsulation of drugs in oil-in-water (O/W) microemulsions, and dispersion of the microemulsions in p-HEMA gels. Microemulsions are thermodynamically stable isotropic dispersions of nano-size drops of oil in water stabilized by surfactants, and these are an effective vehicle for encapsulating a hydrophobic drug due to the large solubility of these drugs in the oil phase (Arriagada and Osseo-Asare, 1999).

2. Materials and methods

2.1. Materials

HEMA monomer was purchased from Sigma Chemicals (St Louis, MO); ethylene glycol dimethacrylate (EGDMA), azobis-*iso*-butrylonitrile (AIBN), Brij 97, Tween 80 and octadecyltrimethoxysilane (OTMS) from Aldrich Chemicals (Milwaukee, WI) and hexadecane and hydrochloric acid (HCl) were purchased from Fisher (Pittsburgh, PA). Danisco Cultor, USA, kindly provided Panodan SDK. All the other chemicals were of reagent grade. All the chemicals were used without further purification.

2.2. Synthesis methods

2.2.1. Synthesis of microemulsions

Four kinds of microemulsions were synthesized for subsequent entrapment in the p-HEMA hydrogel.

These are referred to as Type 1, Type 2, Type 3 and Type 4 microemulsions.

To synthesize the Type 1 microemulsion, Tween 80 was dissolved in a 2% NaCl solution with continuous heating and stirring to form a 30% (w/w) solution. Separately, a solution of canola oil and Panodan SDK in a 1.5:1.0 (w/w) ratio was prepared. Next, 14 g of the Tween 80 solution was mixed with 2.5 g of the canola oil solution, and the mixture was heated at 100 °C with continuous stirring at 1000 rpm, until it got clear.

The Type 2 microemulsion was synthesized by adding 40 mg of OTMS to 16.5 g of the Type 1 mixture. The mixture was then heated at 100 °C with continuous stirring at 1000 rpm until the solution became transparent. Since OTMS is an amphiphilic molecule, it is expected to accumulate at the oil/water interface during emulsification. To polymerize the OTMS on the surface, 0.61 g of 1N HCl solution was added for each gram of freshly prepared microemulsion. The addition of HCl resulted in hydrolysis of the OTMS molecules followed by condensation on the surface of the oil drops, thus forming a silica shell. The hydrolysis and condensation reactions were performed in a water bath at a temperature of 60 °C for 6 h.

To synthesize the Type 3 microemulsion, 0.12 g of hexadecane was added to a mixture of 10 g water and 1.5 g of Brij 97. The mixture was then heated at 60 °C and simultaneously stirred at 1000 rpm until it became clear. This resulted in the formation of a 1.05% oil microemulsion. In some experiments the oil fraction was increased to 5.6% to increase the drug loading in the gels. A silica shell was deposited on the Type 3 microemulsion drops by following the procedure identical to the one used to deposit the silica shell on the Type 1 microemulsion drops. The silica-stabilized Type 3 microemulsion is referred to as a Type 4 microemulsion. The components of the microemulsions described above are listed in Table 1.

2.2.2. Synthesis of particle-loaded p-HEMA gels

The particle-loaded p-HEMA hydrogels were synthesized by free radical solution polymerization of the monomer with chemical initiation. The cross-linker EGDMA (37 μl) and the monomer HEMA (10 ml) were added to 7.4 ml of one of the microemulsions described above. The solution was degassed by bubbling nitrogen for 30 min. This reduced the dissolved oxygen in the mixture. Next, 32 mg of the initiator AIBN were combined with 25 ml of the polymerization mixture and the resulting solution was poured in between two glass plates that were separated from each other with soft plastic tubing. The polymerization reaction was performed in an oven at 60 °C for 24 h. The hydrogels loaded with the Type 1–4 microemulsions are referred to as Type 1–4 gels, respectively. The pure p-HEMA gels were synthesized by replacing the microemulsion by an equal volume of DI water.

2.3. Characterization studies

2.3.1. Particle characterization

To determine the particle size, the microemulsions were characterized by light scattering in a Brookhaven Instruments, Zeta Plus particle size analyzer. The Type 4 microemulsions were also characterized by transmission electron microscopy studies.

In the transmission electron microscopy (TEM) experiments, the oil phase of the Type 4 microemulsion (hexadecane) was doped with unsaturated 1-dodecene. The double bond present in 1-dodecene allows the oil phase of the microemulsion to be stained with osmium tetraoxide, OsO_4 (Electron Microscopy Sciences) dye. A drop of the doped microemulsion was placed on a carbon-coated copper grid and left overnight, so that the water could evaporate. Then the copper grid was transferred to a closed container where OsO_4 vapor was allowed to diffuse through the surfactant layer for a period of 4 h, and stain the oil phase of the

Table 1
Components of the microemulsions used in the synthesis of Type 1–4 hydrogels

Microemulsion	Oil phase	Continuous phase	Surfactant	Silica shell?
Type 1	Canola oil	2% NaCl solution	Tween 80 and Panodan SDK	No
Type 2	Canola oil	2% NaCl solution	Tween 80 and Panodan SDK	Yes
Type 3	Hexadecane	Water	Brij 97	No
Type 4	Hexadecane	Water	Brij 97	Yes

microemulsion. The TEM images were obtained using a Hitachi H-7000 TEM at 75 kV.

2.3.2. Gel characterization

The transparency of the hydrogels was measured by light transmittance studies in a Thermospectronic Genesys 10 UV–vis spectrometer at a visible wavelength of 600 nm. A TJEOL JSM6330F field emission scanning electron microscope (SEM) was used to study the microstructure of the drug-laden hydrogels. The samples were kept overnight in a vacuum oven to remove the volatile components from the gel. The dried samples were cracked in liquid nitrogen and the freshly exposed surfaces were studied by the SEM. The lowest possible accelerating voltages were used in the experiments and a very thin carbon coating was applied to prevent charging of the samples. Optical images at 500× magnification were obtained by an Olympus BX60 Optical Microscope (with SPOT RT Digital Camera) both before and after the vacuum treatment to determine if any structural changes occurred during the vacuum drying.

2.3.3. Drug loading into pure p-HEMA gels

A model hydrophobic drug, lidocaine was used in this study. To understand the interaction of the drug with the hydrogel, drug-loading experiments were performed with pure p-HEMA hydrogels. The pure p-HEMA gels synthesized by the procedure described above were first submerged in a beaker containing 40 ml of well-stirred water for a period of 5 days. This was done to ensure the removal of any unreacted monomer from the gels. The rectangular samples were placed on the thin edge so that the two larger surfaces of the samples were in contact with the well-stirred aqueous solution. Mixing experiments with water-soluble dye were performed to ensure that the aqueous solution was well mixed on a time scale of a few seconds. During the period in which the samples were placed in water, the absorbance of water was measured as a function of time with the UV–vis spectrophotometer at a wavelength of 270 nm, and it was determined that it leveled of in a period about 3 days. The gels were then submerged in a well-stirred drug solution at room temperature and at a pH of about 6.5, and the absorbance of the solutions were measured as a function of time to determine the drug concentration. The volume of water was 40 ml; the gel thickness was 1.25 mm for each of the experiments and the gel volume varied between 0.25 and 0.35 ml. The absorbance values were measured by UV–vis spectrophotometer (Thermospectronic Genesys10 UV) at a wavelength of 270 nm. The loading experiments were conducted for four different drug concentrations in the aqueous phase varying from 0.3 to 4.3 mM.

2.3.4. Drug release studies from particle-laden gels

Lidocaine was entrapped in the microemulsion drops by dissolving it in the oil (canola oil or hexadecane) phase before forming the microemulsions. After synthesis of the gels that contained the drug-loaded microemulsion nano-drops, drug release experiments were performed to establish that the trapped drug can diffuse out of the particles. Although lidocaine is hydrophobic, it has a finite solubility in water at the experimental pH of around 6.5, and thus it diffused out of the nanoparticles and through the gel matrix into the water phase. The diffusion process stopped when the concentrations in the beaker, in the gel, and in the particles reached equilibrium. In the drug release experiments, the samples were submerged in a beaker of well stirred water at room temperature and at a pH of 6.5 and aliquots of water were withdrawn at various times; the concentration of the drug in the aliquots was determined in the UV–vis spectrophotometer at a wavelength of 270 nm. Gel samples of rectangular shape with a volume of about 0.3 ml and a thickness ranging from 0.2 to 1.2 mm were used in these experiments. The drug loading in the samples varied and the exact values for each individual experiment are given in Section 3. The volume of water in the beaker was kept substantially higher than the gel volume to ensure that a majority of the drug diffused out into the water. Also, reference hydrogels (i.e., gels that were identical to the samples with the exception that they did not contain any drug) were prepared for use as blanks. The absorbance values of the blanks were attributed to the diffusion of the unreacted monomer and some of the components of the nanoparticles, such as the surfactant and the oil. The diffusive flux of the surfactant and the unreacted monomer from the gel may change on addition of lidocaine to the samples but since at the same concentrations, the absorbance of the surfactants (Brij 97 and Tween 80) at 270 nm is less than 4% of that of the drug lidocaine, the differences in the absorbance between the

samples and the blank can be attributed mainly to the diffusion of the drug. Accordingly, the concentration of the drug in the aqueous solution was calculated by determining the difference in the absorbance between the sample and the blank experiments, and using the calibration curve for lidocaine to relate the absorbance to the concentration.

3. Results and discussion

3.1. Particle size measurements

The Type 1 microemulsion had an average particle diameter of about 14 nm. It was light yellow in color, a condition that may be undesirable for entrapment in contact lenses. After 3 days of shelf storage, the microemulsion started to slowly lose its transparency and became a milky solution due to particle agglomeration. The Type 2 microemulsion also had a slight yellowish color and had a mean particle diameter of 20 nm. It was stable for about 2 weeks of shelf storage. The Type 3 and the Type 4 microemulsions were transparent and colorless and had average particle diameters of 10 and 15 nm, respectively. They both remained stable for about 2 weeks. The particle size distributions for all four types of microemulsions are shown in Fig. 2.

The TEM image of the Type 4 microemulsion is shown in Fig. 3. The figure shows that the particle diameters vary from about 150 to 500 nm. This is surprising since the light scattering studies show particle diameter values of around 15 nm. The discrepancy is perhaps caused by aggregation during the water-evaporation step. Thus, it may be reasonable to expect that the Type 4 microemulsions will partially aggregate during the polymerization.

3.2. Transparency of microemulsion loaded p-HEMA gels

On adding the Type 1 microemulsion to the polymerization mixture, the solution became opaque. This happened because the surfactant Tween 80 is very soluble in the HEMA monomer. Consequently, upon mixing the monomers with the microemulsion, the surfactant molecules desorbed from the oil drops and caused destabilization and aggregation of the oil drops. The aggregation of the nanodrops resulted in the formation of larger oil drops, which scattered light, and caused the loss of transparency. The hydrogels formed by polymerization of this opaque mixture were also opaque and had a transmittance of about 4.4%. The measured value of transmittance for the pure p-HEMA hydrogel of the same thickness and with the same amount of water was about 87% (Table 2).

The Type 2 microemulsion was expected to be more stable due to the silica shell on the surface of the drops. When the Type 2 microemulsion was

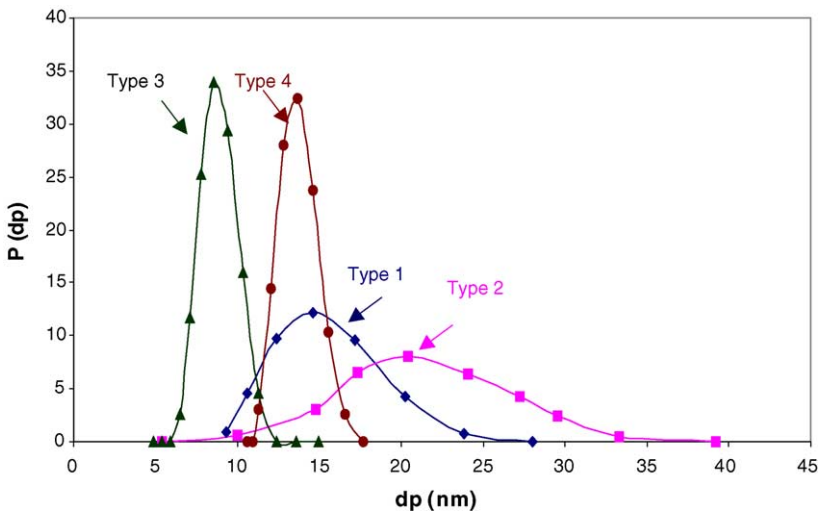

Fig. 2. Particle size distributions for Type 1–4 microemulsions.

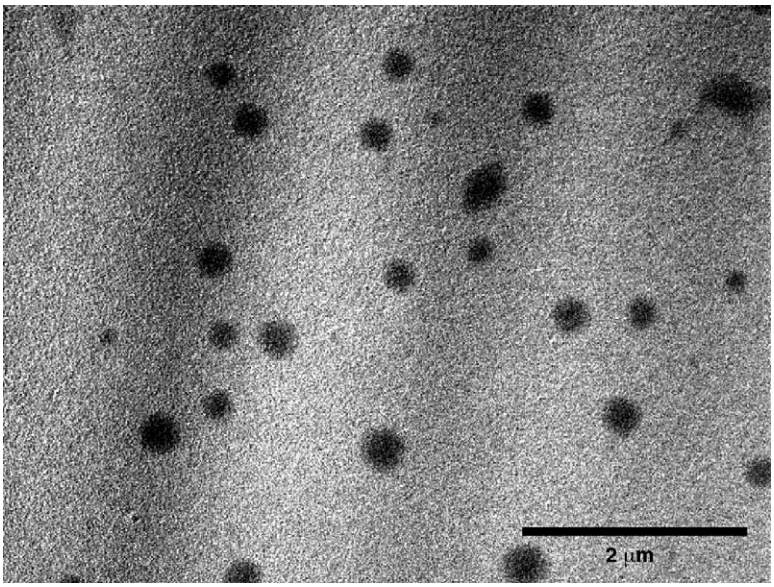

Fig. 3. TEM image of a Type 4 microemulsion.

added to the polymerization mixture, the solution lost some of its transparency but did not turn opaque. This indicated that the addition of OTMS to form the silica shell around the particles helped to reduce the interaction of the surfactant molecules with the monomer. However, it did not prevent the interaction completely. Therefore, there was still some transparency loss, and hydrogels prepared with Type 2 microemulsions had transmittance values of about 19% (Table 2).

To prevent the aggregation of the drops in the polymerizing medium, it was decided to synthesize microemulsions with Brij 97, which is not as soluble in HEMA as Tween 80. When the Type 3 microemulsion was added to the polymerization mixture, the solution had a minimal loss of transparency. The transparency of the hydrogels synthesized with the Type 3 microemulsion was around 66%, which was higher than the transparency of the hydrogels synthesized with the Type 1 and the Type 2 microemulsions, but was still less than the transparency of the pure p-HEMA gels.

Table 2
Transmittance values of the hydrogels loaded with different microemulsion nanodrops and hydrogels with no particles

Hydrogel type	Transmittance (%)
Type 1	4.4
Type 2	19
Type 3	65.6
Type 4	79
p-HEMA (no particles)	87

Transmittance values were obtained at 600 nm for gels with a 1 mm thickness.

Since the Type 2 gels were more transparent than the Type 1 gels, it was expected that the Type 4 microemulsions that have a silica shell around the oil droplets would yield more transparent gels. When this microemulsion was added to the polymerization mixture, no transparency loss was observed. Furthermore, the hydrogels synthesized with Type 4 microemulsion had about 79% transparency, which was close to the 87% transmittance value of the pure p-HEMA hydrogels (Table 2). The difference in the transmittance values for a pure p-HEMA and a Type 4 hydrogel will be smaller for contact lenses which are about 10 times thinner than the lenses that were employed in the transmittance measurements.

3.3. Microstructure of the microemulsion-laden gels

The SEM studies were performed to determine the structure of the microemulsion-laden hydrogels and directly observe the particles entrapped

inside the hydrogel matrix. In these studies, the sample preparation methods can potentially introduce artifacts. To determine the effect of the sample preparation steps, optical microscope images of the hydrogels at 500× magnification both before and after the treatment with liquid nitrogen and vacuum drying were compared. There were no gross differences between the two sets of images, which suggested that the sample preparation step was not introducing major artifacts at a length scale of a micron. However, the sample preparation steps may have altered the detailed structure of the hydrogel at much smaller length scales. The SEM studies were done at two different levels of magnification; some were done at 1000× to see the gross morphology of the gels, and some studies were undertaken at 10k×–60k× magnifications to provide direct evidence of the particle entrapment. These studies are described below.

The SEM image of the cross-section of a pure p-HEMA hydrogel at 1000× magnification appears smooth and non-porous and does not have any grain boundaries (Fig. 4). However, an image of a hydrogel loaded with particles of Type 1 microemulsion at 1000× magnification shows a rough surface with enhanced grain boundaries (Fig. 5). This drastic change in the structure of the hydrogel with the addition of the Type 1 microemulsion occurred due to the breakup of the particles because of the dissolution of the surfactant in the monomer. During free radical solution polymerization of HEMA, small gel domains form early in the polymerization and these domains subsequently grow larger. Eventually, depending on the water fraction, they join to form one contiguous gel (Merkovich et al., 2001). In the polymerization of HEMA in the presence of the Type 1 microemulsion, the oil that was released from the breakup of the particles accumulated in between the growing p-HEMA domains. This led to the enhanced grain boundaries and a rough microstructure (Fig. 5). The phase separation and the highly enhanced grain boundaries caused a refractive index contrast that led to the minimal transparency values for the Type 1 hydrogels.

The SEM image of the Type 2 hydrogel in Fig. 6 shows that it had a different structure than both the pure p-HEMA and the Type 1 hydrogel. The image shows about 2–5 μm size aggregates and holes embedded in a smooth matrix. The differences in the morphology of Type 1 and 2 hydrogels are likely due to the stabilization of the Type 2 particles by the silica shell. It is hypothesized that the silica shell stabilized the particles and

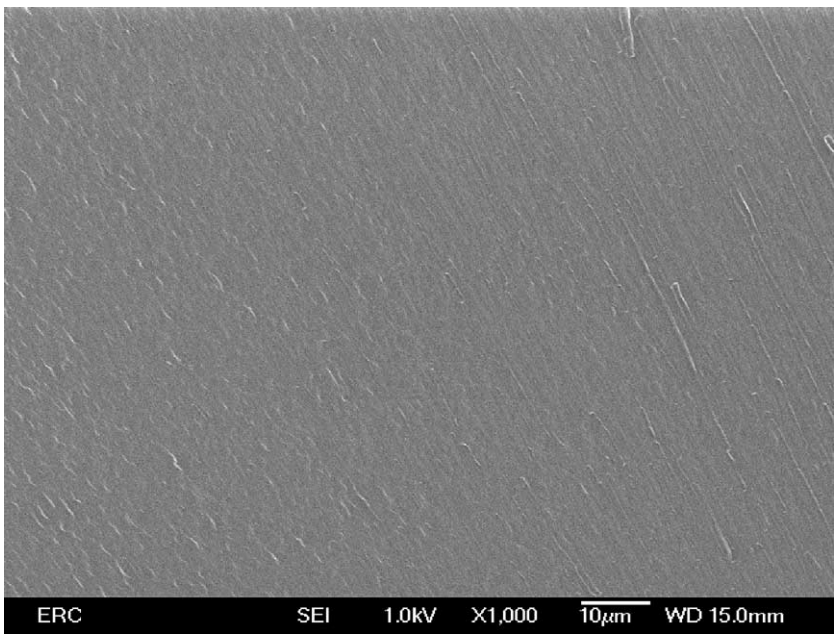

Fig. 4. SEM image of a pure p-HEMA hydrogel at 1000× magnification.

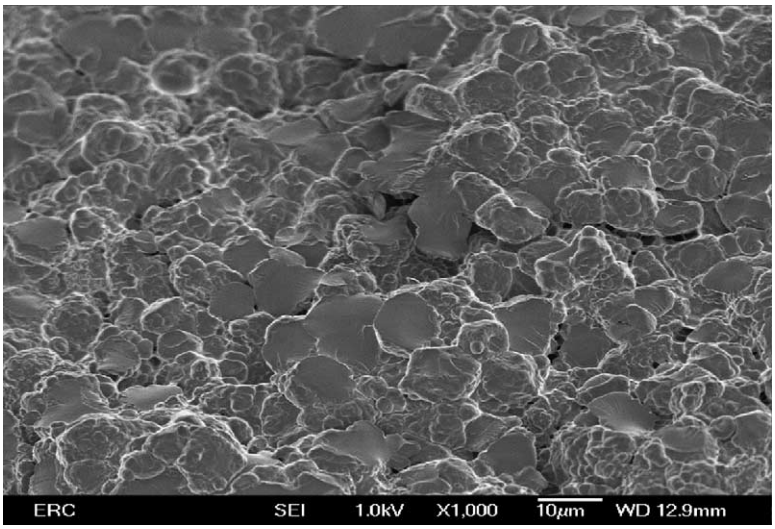

Fig. 5. SEM image of a hydrogel loaded with drug-laden particles of Type 1 microemulsion at 1000× magnification.

prevented particle breakup, but during polymerization the particles aggregated and segregated to form 2–5 μm size clusters. During the cracking of the gel, the cracks perhaps propagated along the surface of the aggregates and thus created a few holes that are visible in the SEM image. The presence of the agglomerates also caused scattering that led to a loss of transparency.

The SEM image of a Type 3 hydrogel looks similar to that of the pure p-HEMA hydrogel with the exception that some grain boundaries are observable in the Type 3 gels (Fig. 7). This implies that the Type 3 particles did not break during the polymerization. The Type 3 particles were stable because the surfactant Brij 97 is less soluble in the polymerizing mixture than Tween 80. The particles also do not aggregate during the polymerization, and thus the gels stay transparent. The SEM images of the Type 4 laden gels (Fig. 8) look similar to the Type 3 and to the pure p-HEMA

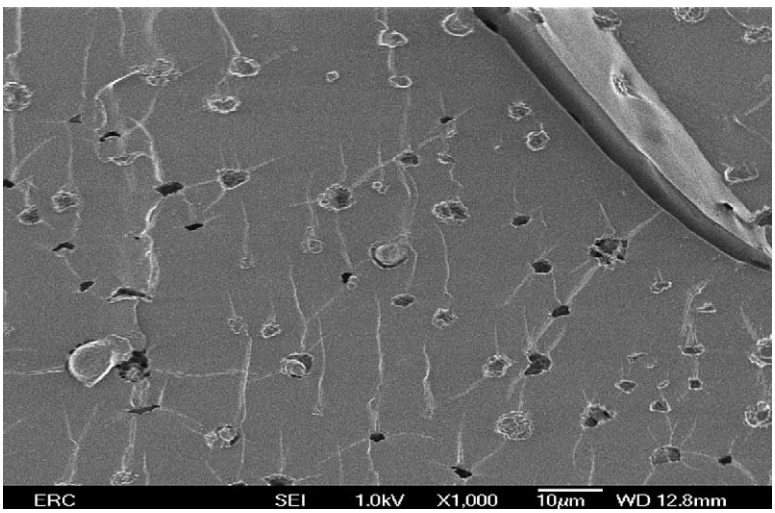

Fig. 6. SEM image of a hydrogel loaded with drug-laden particles of Type 2 microemulsion at 1000× magnification.

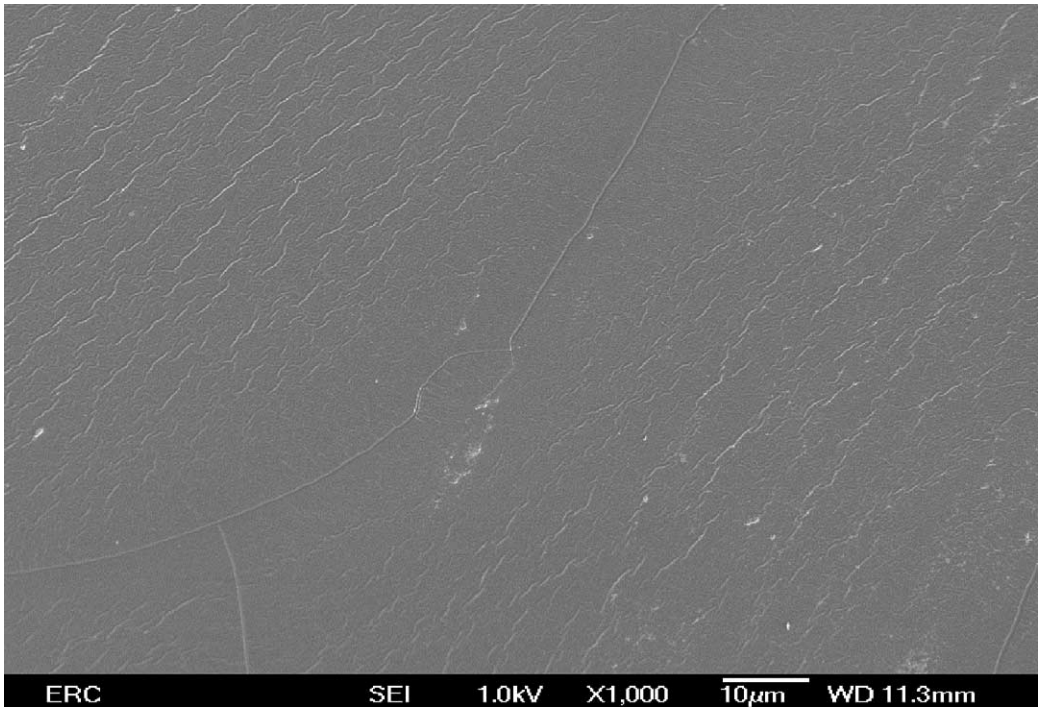

Fig. 7. SEM image of a hydrogel loaded with drug-laden particles of Type 3 microemulsion at 1000× magnification.

gels, which was expected due to the stabilization of the particles by the presence of the silica shell.

The SEM images at higher magnifications provided direct evidence that particles were entrapped in the gel matrix during polymerization (Figs. 9–11). However, the diameters of the particles were different in different types of gels. The sizes of these drop-like structures were about 300–500 nm for Type 1 and 2 gels (Figs. 9 and 10), which was about 20–30 times the size of a single microemulsion droplet. This implies that the particles seen in these figures must be clusters or bigger particles formed by coalescence. Smaller microemulsion-droplet size particles were not observed in these two hydrogels. The SEM images at higher magnifications of Type 4 gels showed the presence of two different types of micron-sized domains. One domain did not contain particles and its morphology looked identical to pure HEMA even at very high magnification (Fig. 12). The other domain showed the presence of isolated and uniformly distributed particles (Fig. 11). The area fraction of the particles in the regions that contained the particles was about $1.6 \pm 0.4\%$. The volume fraction of oil in the Type 4 dried gel was about 0.5%. This suggested that only about 30% of the gel contained the nanoparticles. The particles in Fig. 11 seem elongated, which suggests that these particles were subjected to stresses either during the polymerization process or during the SEM sample preparation process. The area of each particle is about three times the cross-sectional area of the microemulsion drops, which suggests that even the Type 4 particles partially aggregated after the addition of the monomer to the microemulsion.

3.3.1. Proposed mechanism for the particle entrapment

As mentioned above, in free radical polymerization, small gel domains form early in the polymerization and these subsequently grow larger, and eventually depending on the water fraction, join to form one contiguous gel (Merkovich et al., 2001). This nucleation and growth-like mechanism has very important implications in the synthesis of particle-laden gels. When particles are present in the polymerizing mixture, they can either get uniformly distributed in the matrix or get excluded out of the growing HEMA

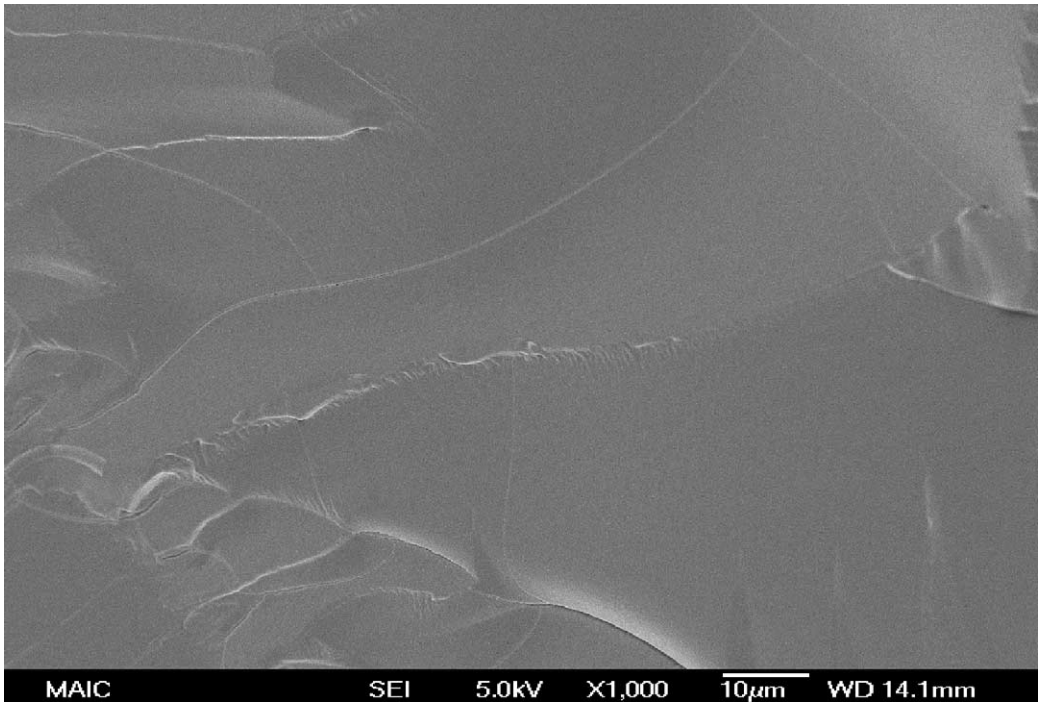

Fig. 8. SEM image of a hydrogel loaded with drug-laden particles of Type 4 microemulsion at 1000× magnification.

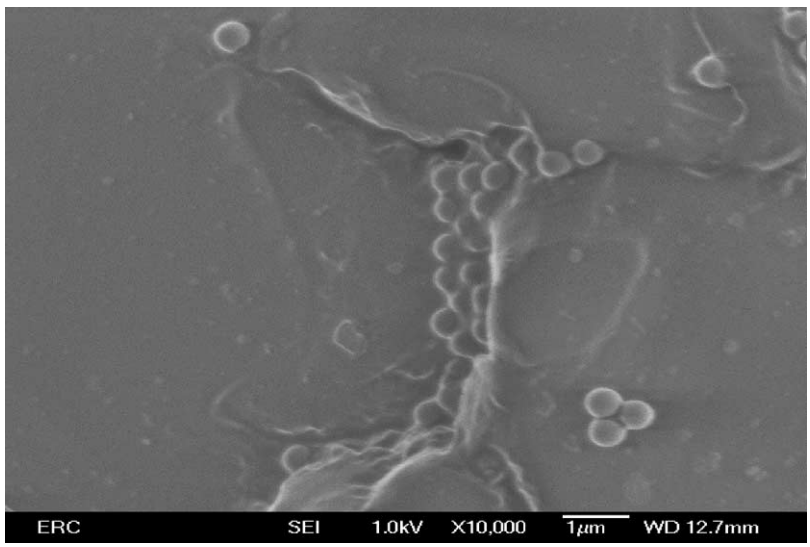

Fig. 9. SEM image of a hydrogel loaded with drug-laden particles of Type 1 microemulsion at 10,000× magnification showing the particles.

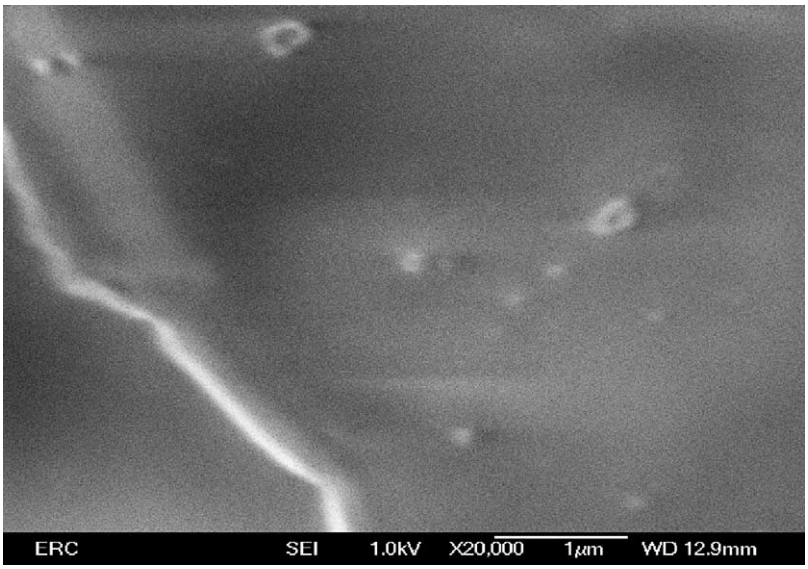

Fig. 10. SEM image of a hydrogel loaded with drug-laden particles of Type 2 microemulsion at 20,000× magnification showing the particles.

grains eventually aggregating at the grain boundaries. To understand the mechanism of entrapment, consider a nanoparticle of diameter D_p and Stokes–Einstein diffusivity $D = k_B T/3\pi\mu D_p$ that is approaching a growing p-HEMA domain (k_B, T and μ are the Boltzmann constant, temperature and viscosity, respectively). If there is no specific interaction between the particle and the gel, the nanoparticle is free to diffuse, so it spends a time τ_d of about D_p^2/D near the growing grain. Since the growing HEMA domain is relatively dense, the particle is expected to not diffuse into the gel. It only gets trapped if the gel grows to encapsulate it before

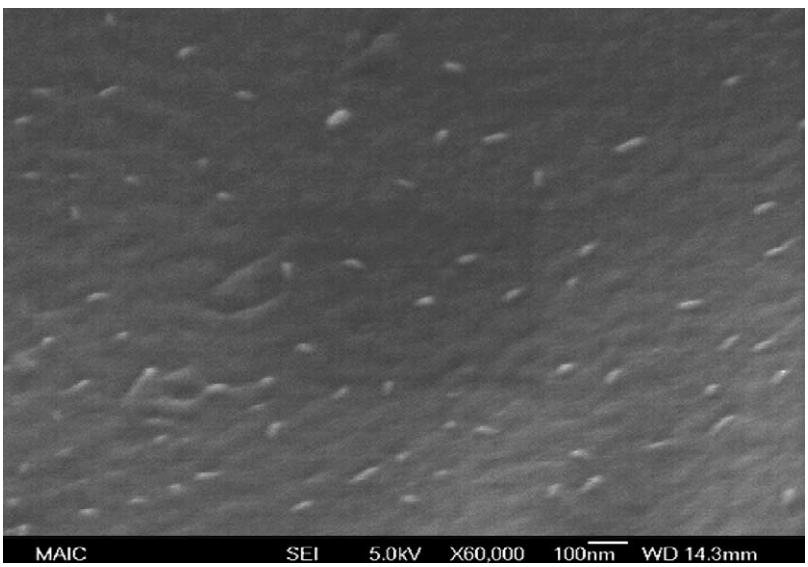

Fig. 11. SEM image of a hydrogel loaded with drug-laden particles of Type 4 microemulsion at 60,000× magnification showing the particles.

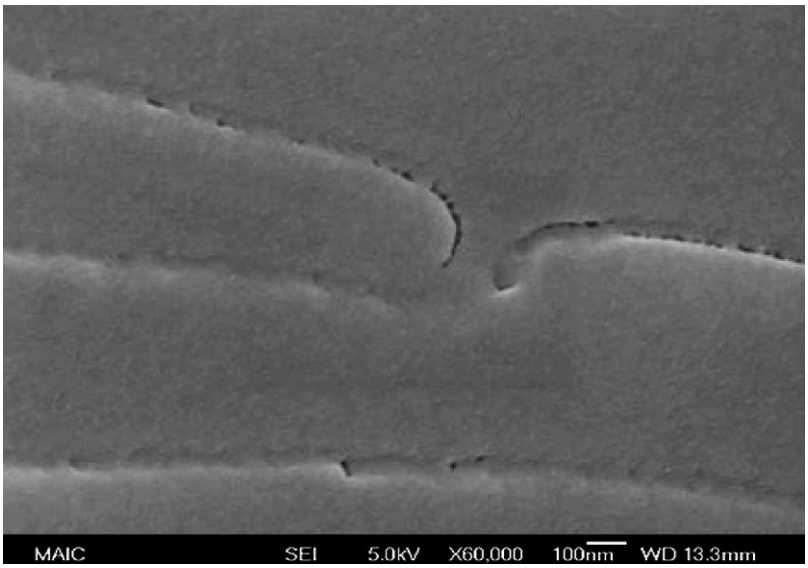

Fig. 12. SEM image of a hydrogel loaded with Type 4 nanoparticles at 60,000× magnification. The image shows a region with no particles.

the particle diffuses away. Let the time required by the grain to grow by a size D_p be τ_g. If $\tau_g \ll \tau_d$ then the particles will get trapped inside the gel. However, if $\tau_g \gg \tau_d$, the nanoparticles will diffuse away from the gel before the gel can grow to trap the particles, resulting in accumulation of the particles in the inter-grain space and eventual segregation at the grain boundaries.

In the scenario in which $\tau_g \gg \tau_d$, the particles do not get trapped in the gel and thus the concentration of the particles in the bulk increases with time. Eventually, the high concentration of the particles in the bulk and, more importantly, the enhancement in viscosity of the fluid due to polymerization in the inter-grain space reduces the particle diffusivity and forces the trapping of the particles in the gel. Assuming Stokes–Einstein diffusivity, a 50 nm particle takes about 0.001 s to diffuse distances of the order of its size. A gel domain grows to a size of a few microns in the reaction time of a few hours. Thus, it seems that in our system $\tau_g \gg \tau_d$, and our proposed mechanism for particle entrapment and development of a two-region microstructure seems reasonable.

3.4. Drug loading and release experiments

The drug release experiments were performed in water with a model drug lidocaine at a pH of about 6.5, which is within the typical range of the pH of the human tear (Carney, 1991). Lidocaine hydrochloride ($C_{14}H_{22}N_2O{\cdot}HCl$) is a water-soluble drug that can be converted to an oil soluble form by reacting it with a base such as sodium hydroxide. The octanol–water partition coefficient for the lidocaine base is 245 (Lee et al., 2001). The solubility of the lidocaine base was measured in the aqueous phase and in the two oils (hexadecane and canola oil) that were used in the microemulsion synthesis. The solubility of lidocaine in hexadecane is 0.04 g/ml at room temperature and 0.056 g/ml at 60 °C. The solubility of the drug in canola oil is 0.064 and 0.074 g/ml at room temperature and 60 °C, respectively. The solubility of lidocaine in water at room temperature and at a pH of 6.5 is 2.7 mg/ml. It was also determined that the elusion time for lidocaine in an HPLC column does not change on exposure to experimental temperatures, which suggests that the drug retains its molecular structure.

Lidocaine is an anti-arrhythmic drug commonly used to restore a regular heartbeat in patients with arrhythmia (Carney, 1991). Lidocaine was used as a model drug in this study because it is inexpensive and available in a pure form. It is contemplated that any of the other ophthalmic drugs including Timolol, a non-selective beta-adrenergic receptor blocking agent that treats glaucoma, Cyclosporin A, a lipophilic cyclic

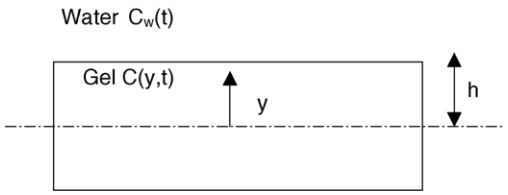

Fig. 13. Schematic illustration of the gel for the drug loading experiments.

polypeptide that has shown promising results in the treatment of dry eye symptoms, hydrophobic steroids such as Prednisolone acetate that are used for treating macular edema, and several other ophthalmic drugs could also be successfully entrapped in nanoparticles and subsequently dispersed in hydrogels. However, different kinds of nanoparticles may need to be used to encapsulate different drugs.

3.4.1. Drug loading into pure p-HEMA gels

A schematic illustration of the gel used in the loading experiments is shown in Fig. 13. The loading experiments were used to determine the partition coefficient, i.e., the ratio of the concentration in the gel and the concentration in the aqueous phase at equilibrium and the diffusion coefficient of the drug in the pure p-HEMA gel. In these experiments the concentration of the drug in water (C_w) was measured as a function of time. At the end of about 4 days equilibrium was established between the gel and the aqueous phase. The mass of the drug taken up by the gel during the loading is equal to $V_w(C_{w,0} - C_{w,f})$, where V_w (=40 ml) is the volume of the aqueous phase, and $C_{w,f}$ and $C_{w,0}$ the final and initial concentrations of the drug in the aqueous phase, respectively. Accordingly, the partition coefficient is defined as

$$K = \frac{V_w(C_{w,0} - C_{w,f})}{V_{gel}C_{w,f}},$$

where V_{gel} is the gel volume. Fig. 14 plots the partition coefficient K as a function of the equilibrium concentration in the water, $C_{w,f}$. The partition coefficient clearly depends on the concentration, and this suggests that the drug interacts with the gel; a fraction of the drug mass in the gel is present in the free form and the remaining is bound to the gel. The binding of the drug to the gel can be modeled as a Langmuir adsorption isotherm, which relates the adsorbed concentration of the drug

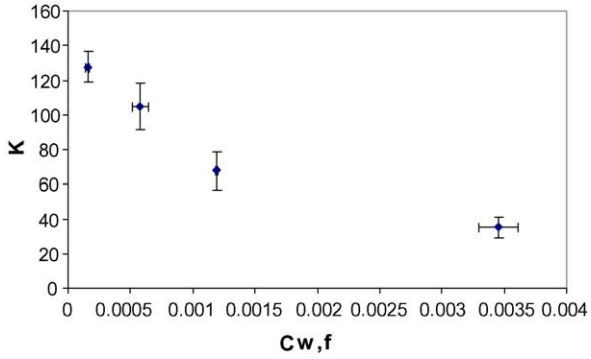

Fig. 14. Effect of the bulk drug concentration on the equilibrium partition coefficient. The error bars represent the standard deviation.

on the gel (Γ) to the free concentration in the aqueous phase inside the gel (C) by the following equation:

$$\Gamma = \frac{\Gamma_\infty C}{k + C} \quad (1)$$

where Γ_∞ is the surface concentration at the maximum packing on the surface and k the ratio of the rate constants for desorption and adsorption of the drug on the HEMA polymer. The total drug content of a gel of volume V_{gel} with a uniform free concentration C is $(S/V)_{gel}V_{gel}\Gamma + fV_{gel}C$, where $(S/V)_{gel}$ is the surface area per volume available for the drug to adsorb and f the fraction of the gel volume that contains water. The value of f, which is essentially the saturation water fraction in the gel, is about 0.4 for pure p-HEMA gels (Peppas, 1987). The mean concentration of the drug in the gel is thus equal to $(S/V)_{gel}\Gamma + fC$. Assuming that at equilibrium the concentration of the drug in the aqueous phase inside the gel is the same as the drug concentration in the bulk water outside the gel ($C = C_{w,f}$), the partition coefficient is given by

$$K = \frac{(S/V)_{gel}\Gamma + fC}{C} \quad (2)$$

Using the Langmuir adsorption isotherm (Eq. (1)), the expression for K becomes

$$K = \left(\frac{S}{V}\right)_{gel}\frac{\Gamma_\infty}{k + C} + f \Rightarrow K - f = \frac{a}{k + C} \quad (3)$$

where $a \equiv (S/V)_{gel}\Gamma_\infty$ and f as mentioned above has a constant value of 0.4. Accordingly, a plot of $1/(K - f)$ versus C is expected to yield a straight line. Fig. 15 shows the same data as in Fig. 14, except that $1/(K - f)$

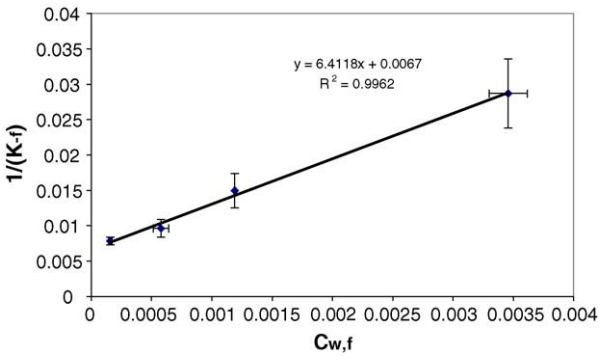

Fig. 15. Linear (Langmuir) fit between the inverse of the partition coefficient and the equilibrium drug concentration in water. The error bars represent the standard deviation.

is plotted as a function of $C = C_{w,f}$. The plot also shows the best fit straight line; the best-fit values of a and k are 0.1560 and 0.001 M, respectively. The good fit between the Langmuir model and the experimental data strongly suggests that the drug indeed adsorbs on the polymer inside the gel.

3.4.2. Dynamics of drug loading into pure p-HEMA hydrogels

Since a major fraction of the drug in the gel is adsorbed on the HEMA polymer, the diffusion equation needs to be modified to include both the bound and the free drug into the equation. The modified form of the diffusion equation is

$$\frac{\partial fC}{\partial t} + \frac{\partial (S/V)_{\text{gel}}\Gamma}{\partial t} = D\frac{\partial^2 C}{\partial y^2} \tag{4}$$

where the two terms on the left account for accumulation in the bulk of the gel and the accumulation of the bound drug, and the term on the right represents the divergence of the diffusive flux of the free drug. It is assumed that the bound drug cannot diffuse, which implies that the surface diffusion has been neglected. In the above equation f has a value of 0.4. Utilizing Eqs. (2) and (3) into (4), one gets

$$\frac{\partial K(C)C}{\partial t} = D\frac{\partial^2 C}{\partial y^2} \tag{5}$$

Substituting K from (3) into the above equation, one gets

$$\frac{\partial}{\partial t}\left(\frac{a}{k+C} + f\right)C = D\frac{\partial^2 C}{\partial y^2} \tag{6}$$

The boundary conditions for the drug loading experiment are

$$\frac{\partial C}{\partial y}(t, y = 0) = 0, \qquad C(t, y = h) = C_{\text{w}} \tag{7}$$

where h is the half-thickness of the gel, the first boundary condition assumes symmetry at the center of the gel and the second boundary condition assumes that the free drug concentration in the gel at the boundary with the fluid is the same as the drug concentration in the fluid.

A mass balance on the fluid in the beaker yields

$$V_{\text{w}}\frac{\text{d}C_{\text{w}}}{\text{d}t} = -2DA_{\text{gel}}\frac{\partial C}{\partial y}|_{y=h} \tag{8}$$

Finally the initial conditions for the drug loading experiments are

$$C(y, t = 0) = 0, \qquad C_{\text{w}}(t = 0) = C_{\text{w},0} \tag{9}$$

In the drug loading experiments, the dynamic drug concentration in the aqueous phase was measured, and the data can be fitted to the above model to determine the diffusion coefficient of the drug in the gel. The model described above was solved by an implicit finite-difference scheme with backward differencing in time and center differencing in space. The finite difference scheme had 21 spatial nodes and a dimensionless time step ($D\Delta t/h^2$) of 0.02. The nonlinear differential equation was linearized at each time step around an approximate guess solution and the deviation from the guess solution was calculated by the finite difference method. The guess solution was then updated and the procedure was repeated till the convergence was achieved. The simulations were checked to ensure grid independence and mass conservation. The error between the model prediction and the experimental data was defined as

$$\frac{\sqrt{\sum (C_{\text{w}} - C_{\text{w,ex}})^2/N}}{\sum C_{\text{w,ex}}/N} \tag{10}$$

where C_{w} is the predicted concentration in the water, $C_{\text{w,ex}}$ the experimental concentration, and the sum is carried over all the experimental data points.

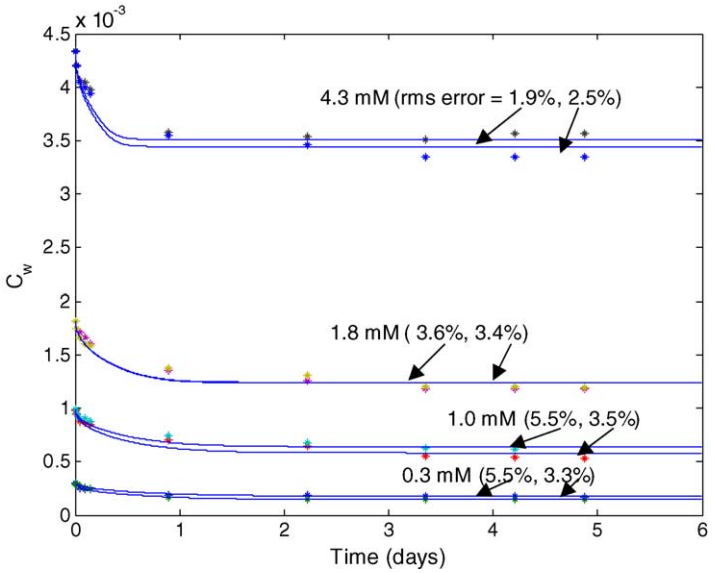

Fig. 16. Comparison of the model prediction and experimental data for drug uptake by a pure p-HEMA gel soaked in drug solution. Initial drug concentrations in the aqueous phase and rms errors in the fit are indicated on the figure.

The drug loading experiments were conducted with four different initial concentrations ($C_{w,i} = 0.0003$, 0.0010, 0.0018 and 0.0043 M). The best-fit value of D was obtained by minimizing the maximum of the error for the set of eight experiments; two runs corresponding to each of the four concentrations. The error minimization was performed by using the function 'fmins' in MATLAB, which determines a local minimum of a function. The value of D obtained by the fit was 2.03×10^{-10} m^2/s. Fig. 16 plots the experimental profiles and also the profiles predicted by the model developed above. The eight experimental curves correspond to two runs for each of the four concentrations. The two theoretical curves for the same concentration are different due to the different gel volumes. The theoretical predictions match the experimental data well; the ratio of the rms error to the mean vary from 1.9 to 5.5% and are noted in the figure caption.

3.4.3. Drug release studies from microemulsion-laden gels

The results of drug release studies from the microemulsion-laden gels are discussed below for the Type 2–4 gels. The drug release studies were not performed on the Type 1 gels because a majority of the particles broke (Fig. 5), and thus some oil leaked out from the samples during the polymerization.

The experimental error in the data described below was estimated by reproducing a select number of experiments. The experimental error was determined to be about ±7%.

3.4.3.1. Drug release from Type 3 gels. Fig. 17 shows the drug release data obtained for the Type 3 hydrogels synthesized with three different drug concentrations; the gels contained 0.31, 0.45 and 2.05 mg of lidocaine base for each gram of hydrogel. The lower two drug loadings were obtained by changing the drug concentration in the oil phase of the microemulsion with 1.1% oil and the highest loading was obtained by preparing the Type 3 microemulsion with 5.6% oil. At the end of the 9-day period, about 95% of the entrapped drug was released into water for each hydrogel. The drug release rates were similar for the three gels, except that the gel that was loaded with the 5.6% oil microemulsion exhibited a much larger initial burst release than the other two gels. The initial burst accounted for about 30% of the total release for the gel with 5.6% oil microemulsion and for about 10% for the other two gels. It is

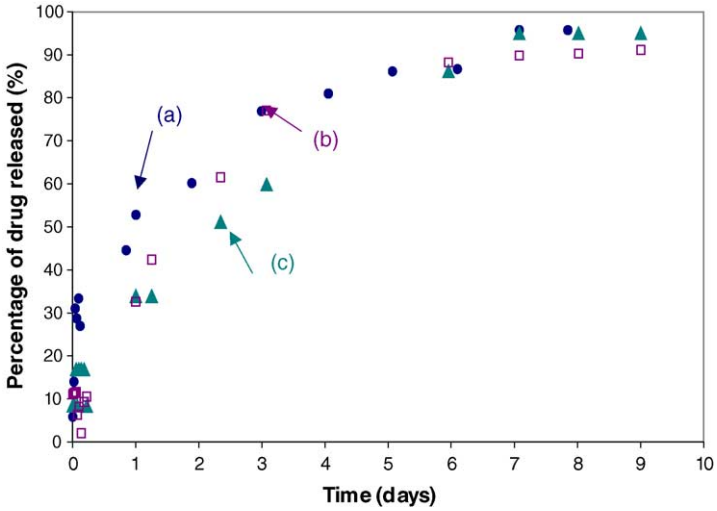

Fig. 17. Percentage drug release from a Type 3 hydrogel initially loaded with (a) 2.05, (b) 0.45 and (c) 0.31 mg lidocaine/g hydrogel.

speculated that the initial burst arose due to the drug that was present in the gel but was outside the particles. Perhaps the increased oil loading reduced the stability of the microemulsions and thus more drops broke during the polymerization, which led to the larger burst effect for the 5.6% microemulsions.

3.4.3.2. Drug release from Type 4 gels. Fig. 18 shows the drug release profiles of two gels loaded with the Type 4 microemulsion. In the figure, the percentage release of the drug is plotted as a function of time for two gels of different thicknesses. As can be seen in the figure, the release profiles are relatively similar for the

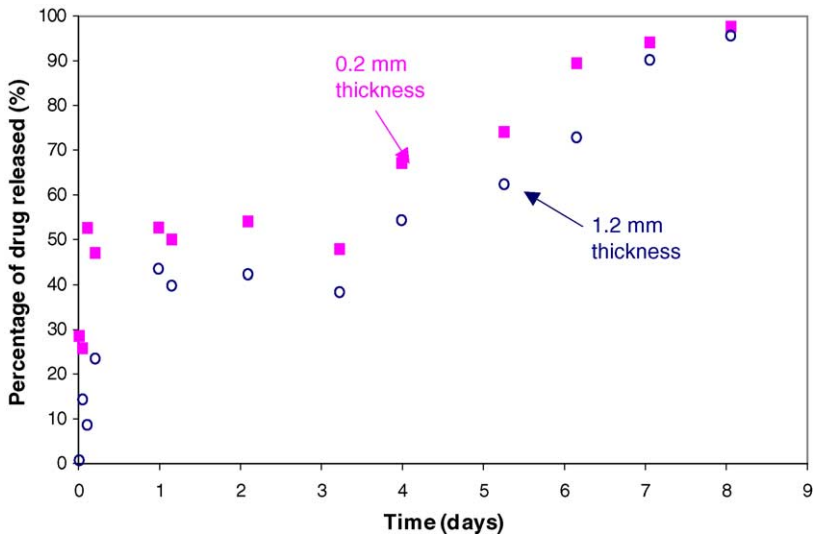

Fig. 18. Percentage drug release from Type 4 hydrogels with different thicknesses. Initial drug loading in both the gels was 1.2 mg lidocaine/g hydrogel.

1.2 mm thick and for the 0.2 mm thick gels, except in the early stages.

The drug release profiles for the Type 4 gels of 0.2 and 1.2 mm thicknesses showed an initial burst of drug release. As shown in the figure, about 50% of the entrapped drug diffused out of the Type 4 gels in the first day for the 1.2 mm thick lens and in the first few hours for the 0.2 mm thick lens. The strong dependence of the duration of the initial burst on the gel thickness suggests that the initial burst was perhaps due to the diffusion of the drug that was present in the gel but was outside the particles. The drug molecules that were entrapped inside the particles encountered the extra resistance offered by the surfactant-covered microemulsion drop, and thus these molecules diffused out of the gel on a longer time scale. The initial burst in the Type 4 gels was larger than that in Type 3 gels because the Type 4 microemulsions were synthesized under acidic conditions, and since the solubility of lidocaine in water is much higher at a lower pH, a larger fraction of the drug diffused out of the particles during the polymerization.

Also, the drug release profiles for the Type 4 gels exhibited a delay of about 3.5 days during which there was negligible drug release after the initial burst. This delay is evident in Fig. 18 for the 1.2 and 0.2 mm thick gels. The delay was absent in the Type 3 gels (Fig. 17). This suggested that the delay might be due to the silica shell deposited on the surface of the Type 4 microemulsions. However, more experiments need to be performed to conclusively determine the cause of the delay.

3.4.3.3. Drug release from Type 2 gels. Fig. 19 compares the drug release profiles for the Type 2 and Type 4 hydrogels. In the figure, the percentage of the initial drug loading released by the gels is plotted as a function of time. The data shows that the release profiles were similar for the Type 2 and Type 4 particles. This result contrasts with the transparency measurements. However, the SEM images showed that the Type 2 particles do not break; they simply aggregate during the polymerization and the aggregation reduces the transparency but does not affect the drug release profiles.

The data discussed above suggests that during the polymerization, a fraction of the drug came out of the particles either by diffusion or due to particle breakup, and this fraction diffused out of the gel faster because the only resistance to the drug transport was diffusion through the gel matrix. The fraction of the drug that was trapped inside the particles diffused out on a slower time scale because of the extra resistance offered by the surfactant-covered interface of the oil drops.

3.4.4. Model of drug release from microemulsion-laden gels

As shown by the studies on lidocaine loading into the pure p-HEMA gels, the process of lidocaine diffusion in the p-HEMA gels is complex due to the adsorption of the drug molecules on the polymer matrix. This process becomes more complicated in the presence of microemulsions. First, as mentioned above the drug that is present inside the microemulsion drops

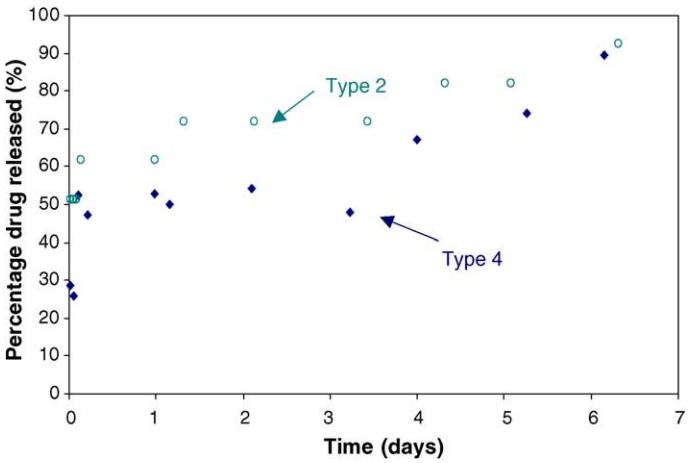

Fig. 19. Comparison of the percentage drug release from 0.2 mm thick Type 2 and Type 4 hydrogels. Initial drug loadings for the Type 4 and Type 2 gels were 1.2 and 2.2 mg lidocaine/g hydrogel, respectively.

encounters an extra resistance offered to diffusion by the surfactant covered drop surface. Secondly, the surfactant molecules are soluble in HEMA, and thus, on the addition of HEMA monomer to the microemulsion, some surfactant molecules dissolve in the HEMA solution. After polymerization, these surfactant molecules are expected to adsorb on the surface of the HEMA matrix. Thus, the drug has to compete with the surfactant molecules for adsorption on the HEMA matrix. In order to develop a model for lidocaine release from microemulsion-laden HEMA gels, one has to develop a model for multi-component (surfactant and drug) adsorption on the p-HEMA matrix. Additionally one has to determine the diffusivity of the surfactant and the drug lidocaine in the microemulsion-laden gels. This complex model can be considerably simplified by assuming that the surface of the HEMA matrix is saturated with the surfactant, and thus the adsorption of the drug lidocaine to the HEMA matrix can be neglected. This assumption is supported by the fact that the amount of the surfactant in the gel is about 100 times than that of the amount of the drug lidocaine. Also in the results discussed above, almost 95% of lidocaine diffused out of the gels, which suggests that only a negligible amount stayed adsorbed inside the gels. However, further experiments are needed to determine the validity of this assumption.

If the adsorption of the drug is neglected, its transport through the gel can be modeled by the diffusion equation. Below a simple model based on the mechanism described above is developed and the experimental results are compared with the model predictions. The model proposed below also assumes that the time scales for release of the drug lidocaine from the particles is much slower than the time scale for diffusion through the gel, and thus the drug released by the particles can be neglected while determining the flux of the drug trapped directly in the hydrogel. The time scale of release is long for both Type 3 and 4 microemulsions due to the resistance offered by the tightly packed surfactant layers. The silica shell increases the resistance further for the Type 4 gels. While determining the flux of the drug that was trapped inside the particles, the resistance offered by the gel is neglected, which is consistent with the above assumption. These two assumptions are consistent with the data reported above which shows that the initial release occurs rapidly.

3.4.4.1. Release of the drug trapped directly in the gel. The geometry for the release experiments from microemulsion-laden gels is the same as that for the drug loading studies for pure p-HEMA gels (Fig. 13). Based on the assumptions stated above, the release of the drug directly trapped in the hydrogel is governed by the diffusion equation:

$$\frac{\partial C}{\partial t} = D\frac{\partial^2 C}{\partial y^2} \tag{11}$$

where C is the concentration of the drug in the gel and D the diffusion coefficient of lidocaine in the microemulsion-laden p-HEMA gel. The value of D in microemulsion-laden gels may be different than that in pure p-HEMA gels; the presence of microemulsions may alter the tortuosity of the gels and also the presence of the surfactant monomer in the aqueous phase inside the gel will increase the viscosity, which will reduce the diffusion coefficient. Accordingly, the value of D for the microemulsion-laden gels was obtained by fitting the initial burst release data to the diffusion model. The diffusion equation is subjected to the following initial and boundary conditions:

$$C(t = 0, y) = C_0 \tag{12}$$

$$\frac{\partial C}{\partial y}(t, y = 0) = 0 \tag{13}$$

$$C(t, y = h) = 0 \tag{14}$$

where C_0 is the initial concentration in the gel and h the half thickness of the gel. The first boundary condition (Eq. (13)) assumes symmetry and the second boundary condition (Eq. (14)) assumes equilibrium between the gel concentration at the boundaries and the concentration in the beaker, which was almost zero due to the large volume of water in the beaker. The solution to the above set of the differential equation and the boundary conditions is

$$C = \sum_{n=0}^{\infty} \frac{4(-1)^n C_0}{(2n+1)\pi} \cos\left(\frac{(2n+1)\pi y}{2h}\right) \times \exp\left(-\left(\frac{(2n+1)^2\pi^2 Dt}{4h^2}\right)\right) \tag{15}$$

The total amount of drug released from the gel can be calculated as

$$M(t) = M_{0,g} - 2A_{gel}\int_0^h C\,dy \quad (16)$$

where $M_{0,g}$ (=C_0V_{gel}) is the initial amount of the drug trapped in the gel outside the particles and A_{gel} the cross-sectional area. Therefore $M(t)/M_{0,g}$ is given by

$$\frac{M(t)}{M_{0,g}} = 1 - \sum \frac{8}{(2n+1)^2\pi^2} e^{-((2n+1)(\pi/2h))^2 Dt} \quad (17)$$

3.4.4.2. Release of the drug trapped inside the particles. The release of the drug from the particles is simply modeled by the following equation:

$$V_P\frac{dC_P}{dt} = -S_P k C_P \quad (18)$$

where V_P and S_P are the volume and the surface area of a particle, C_P the concentration of the drug inside the particle, and k the mass transfer coefficient for drug transport across the particle surface, which is assumed to remain unchanged with time. The above expression assumes that the time scale for drug release from the particle (=R_P/k) is much larger than the time scale for diffusion through the gel (=h^2/D) and thus the gel concentration is almost zero. Note that R_P is the radius of the particle. Eq. (18) can be integrated to give

$$C_P = C_{P,0}\, e^{-(R_P t/3k)} \quad (19)$$

where $C_{P,0}$ is the initial concentration of the drug in the particles. The total amount of drug released from the particles is

$$M_P(t) = NV_P(C_{P,0} - C_P) = NV_P C_{P,0}(1 - e^{-(R_P t/3k)})$$
$$= M_{0,P}(1 - e^{-(R_P t/3k)}) \quad (20)$$

where N is the number of particles in the gel and $M_{0,P}$ the mass of the drug that was trapped inside the particles. On combining Eqs. (17) and (20) one gets

$$M(t) = M_{0,g}\sum \frac{8}{(2n+1)^2\pi^2}(1 - e^{-((2n+1)(\pi/2h))^2 Dt})$$
$$+ M_{0,P}(1 - e^{-(R_P t/3k)}) \quad (21)$$

The above equation has four unknown parameters: D, $R_P/3k$, $M_{0,P}$ and $M_{0,g}$. However, the sum of $M_{0,P}$ and $M_{0,g}$ is simply equal to the total mass of the entrapped drug (M_0) which is known. The unknown parameters are used to fit the experimental data to the model.s

3.4.4.3. Comparison of model predictions with experimental results.

3.4.4.3.1. Comparison for Type 3 gels. In the Type 3 gels that were synthesized with the 1.1% microemulsion, there was only a small initial burst release and $M_{0,g}$ is assumed to be zero. Thus the only unknown parameter was $3k/R_P$. The drug release data for the drug loading of a 0.45 mg/g was used to obtain the best fit value of $R_P/3k$ (=2.4 days), and then the same value of R/k was used to determine the drug release curves for the loading of 0.31 and 2.05 mg/g. Since the gels with the 2.05 mg/g loading that contained the 5.6% Type 3 microemulsion showed a large initial burst which removed 0.6 mg/g of the drug, it was assumed that $M_{0,P}$ and $M_{0,g}$ are 1.45 and 0.6 mg/g, respectively. The experimental data was fitted to the model developed above to yield the best-fit value of D (=6×10^{-11} m^2/s) for the Type 3 microemulsions. The best-fits were performed by minimizing the function given in Eq. (10) which is the ratio of the mean square error and the mean. The comparison between the experimental data and the model predictions (Eq. (21)) are shown in Fig. 20.

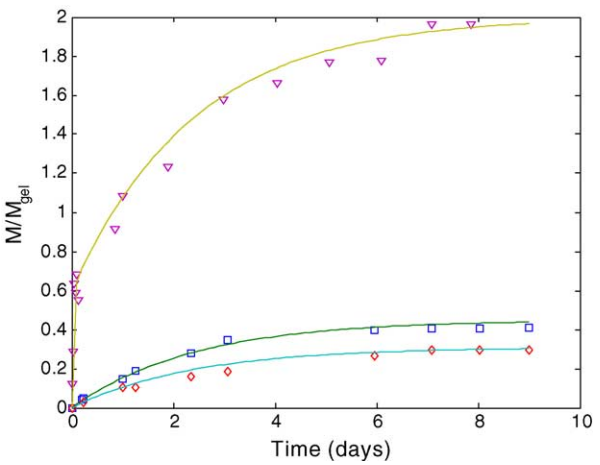

Fig. 20. Comparison of the Type 3 experimental data with the model based on Eq. (21) (solid lines). The mass of drug released per mass of dry gel is plotted on the y-axis. The loadings in the three sets of data were 2.05 (inverted triangles), 0.45 (squares) and 0.31 mg (diamonds) for each gram of hydrogel. The rms error for the fits were 7 (inverted triangles), 6.9 (squares) and 10.8% (diamonds) of the respective mean values.

In Fig. 20 the amount of drug released by the gel per unit mass of the dry gel (M/M_{gel}) is plotted as a function of time instead of plotting the fraction of drug released so that the scales of the curves are different and thus they are clearly distinguishable from each other. The rms errors in the fit were 7, 6.9 and 10.8% of the mean values for the 2.05, 0.45 and 0.31 mg/g loadings, respectively.

3.4.4.3.2. Comparison for the Type 4 gels. As mentioned above, the drug release data for the Type 4 gels exhibited a delay of about 3.5 days after the initial burst. It is speculated that the presence of the silica shell prevents the drug from diffusing out of the oil drops and the delay corresponds to the time in which the silica shell gets destroyed. To incorporate the delay, Eq. (21) was empirically modified to the following form:

$$M(t) = M_{0,g} \sum \frac{8}{(2n+1)^2\pi^2}(1 - e^{-((2n+1)(\pi/2h))^2 Dt}) + M_{0,P}(1 - e^{-(R_P(t-t_{delay})/3k)})u(t - t_{delay}) \quad (22)$$

where t_{delay} is the delay period which was fixed to be 3.4 days and u($t - t_{delay}$) is the step function which is equal to 0 for $t < t_{delay}$ and is equal to 1, otherwise. Also, for the release from the Type 4 gels $M_{0,P} = 0.55$ mg/g of gel for the 0.2 mm gel, $M_{0,P} = 0.45$ mg/g of gel for the 1.1 mm gel, and $M_0 = 1.2$ mg/g for both the gels. The release data for the 1.1 mm thick gel was fitted to the model to obtain the value of D ($=7 \times 10^{-12}$ m^2/s). The value of D is significantly less for the Type 4 gels than the Type 3 gels. The smaller diffusivity may be due to the presence of very small silica grains in the pores of the gel. The detailed mechanisms by which the silica shell affects the drug release from the microemulsion-laden gels will be explored in the future. Fig. 21 shows the comparison between the model and the experimental results. In these plots the same value of $3k/R_P$ was used as obtained above for the Type 3 gels. The rms errors for the fits are 8.39 and 11.5% of the mean for the 0.2 and 1.1 mm gels, respectively.

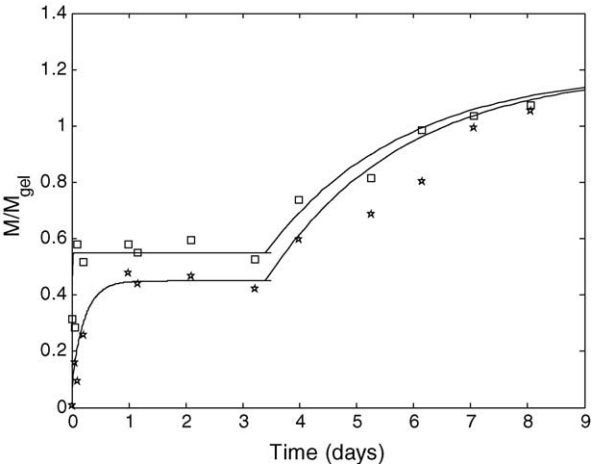

Fig. 21. Comparison of the experimental drug release data with the model based on Eq. (22) (solid lines) for two Type 4 gels of two different thicknesses: 0.2 (squares) and 1.2 mm (stars). The mass of drug released per mass of dry gel is plotted on the *y*-axis. The initial drug loading in both gels was 1.2 mg lidocaine/g hydrogel. The rms errors for the fits are 8.39 and 11.5% of the mean for the 0.2 and 1.2 mm gels, respectively.

3.4.5. Drug loading in a contact lens

The above results show that 1 mm thick hydrogels can be loaded with nanoparticles to deliver drug for several days. However, the drug release rates from contact lenses in the eyes will be different than those from our gels into a well-stirred beaker. The usual starting dose of timolol (Timoptic®) which is a hydrophobic ophthalmic drug is one drop of 0.25% timolol maleate in the affected eye(s) twice a day. Assuming a volume of 25 μl for each drop, the daily dosage of timolol is 0.125 mg each day. Only about 5% of this amount actually reaches the cornea. Thus, the dosage that needs to be delivered to the cornea is about 0.0063 mg each day. At a loading of 1.2 mg of drug per gram of gel, which was the maximum loading in the Type 4 gels, a contact lens can contain about 0.024 mg of drug. The Type 3 gels have slightly smaller transparencies but these gels can be loaded with twice the amount of drug in the Type 4 gels. This is due to the fact that the total amount of microemulsion that can be added to the polymerizing mixture is limited to about 40% and the oil fraction in the Type 4 systems is about half that of the oil fraction in the Type 3 systems due to the addition of the 1N hydrochloric acid to the microemulsion. Thus, a contact lens fabricated out of the Type 4 and the Type 3 gels can contain enough amount of drug to last about 4 and 8 days, respectively. However, a fraction of the drug released by the lens will still be lost due to tear drainage, particularly due to diffusion into the pre-lens tear film and absorption through the conjunctiva. Modeling and

in vivo experiments need to be performed to determine the fraction of the entrapped drug that will enter the cornea.

4. Conclusions

Drug release studies and SEM pictures showed that drug-filled nanoparticles were successfully entrapped in the p-HEMA hydrogel matrices. The hydrogels loaded with the Type 1 and Type 2 particles were opaque due to the destabilization and/or aggregation during polymerization. The microstructures of the Type 3 and Type 4 gels were very similar to the microstructure of the pure p-HEMA gels, and accordingly, the Type 3 and Type 4 gels were transparent. The Type 3 and Type 4 gels can supply drugs at rates comparable to the therapeutic rates for about 4–8 days. The drug delivery from the Type 4 gels exhibited a large burst release, which occurred due to the diffusion of the drug that was present outside the particles. The burst drug release was controlled by diffusion through the gel and the long time release was controlled by diffusion across the surfactant-covered interface of the microemulsion drops. The drug release rates scaled linearly with the concentration of the drug in the oil phase. The diffusivity of the drug in the microemulsion-laden gels was much less in the Type 4 gels than that in the Type 3 gels. Also, the presence of the silica shell on the Type 4 particles introduced a delay period during which there was negligible drug release. The time scale for the subsequent drug release from the Type 4 particles was about the same as that for the Type 3 particles, which suggests that the silica shell breaks down during the delay period.

The main drawback of drug delivery by the nanoparticle-laden gels is the decaying release rates. However, this release profile is still an improvement over the bolus dosage introduced as drops. Furthermore, these drug-laden lenses need to be stored in a pouch saturated with the drug to eliminate drug loss during storage. Designing ‘smart’ particles that respond to pH or temperature change and release drug only in the eye could also eliminate this problem. Also animal testing needs to be done to establish the safety of the components of the microemulsions because the components used in our current study have not been used previously in eyes.

Acknowledgements

The authors gratefully acknowledge Dr. Dinesh O. Shah and Dr. Manoj Varshney for their valuable help in microemulsion synthesis and Kerry Seibein for her help in the SEM studies. The authors also thank Alex Jovanovich for his help in the TEM experiments.

The authors also acknowledge the financial support of the Engineering Research Center (ERC) for Particle Science and Technology at the University of Florida, The National Science Foundation (NSF grant EEC-94-02989), and the Industrial Partners of the ERC for support of this research. Any opinions, findings and conclusions or recommendations expressed in this material are those of the author(s) and do not necessarily reflect those of the National Science Foundation.

Finally the authors thank the reviewers for their detailed and very helpful comments on the manuscript.

References

Arriagada, F.J., Osseo-Asare, K., 1999. Synthesis of nanosize silica in a nonionic water-in-oil microemulsion: effects of the water/surfactant molar ratio and ammonia concentration. J. Colloid Interf. Sci. 211, 210–220.

Arthur, B.W., Hay, G.J., Wasan, S.M., Willis, W.E., 1983. Ultrastructural effects of topical timolol on rabbit cornea. Arch. Ophthalmol. 10, 1607–1610.

Bourlais, C.L., Acar, L., Zia, H., Sado, P.A., Needham, T., Leverge, R., 1998. Ophthalmic drug delivery systems. Prog. Retinal Eye Res. 17, 33–58.

Carney, L.G., 1991. Considerations in contact lens use under adverse conditions. In: Proceedings of a Symposium on Environmental Conditions and Tear Chemistry. The National Academies Press, pp. 34–37.

Colombo, P., Bettini, R., Peppas, N.A., 1999. Observation of swelling process and diffusion front position during swelling in hydroxypropyl methyl cellulose (HPMC) matrices containing a soluble drug. J. Contr. Rel. 61, 83–91.

Creech, J.L., Chauhan, A., Radke, C.J., 2001. Dispersive mixing in the posterior tear film under a soft contact lens. I&EC Res. 40, 3015–3026.

Elisseeff, J., McIntosh, W., Anseth, K., Riley, S., Ragan, P., Langer, R., 2000. Photoencapsulation of chondrocytes in poly(ethylene oxide)-based semi-interpenetrating networks. J. Biomed. Mater. Res. 51, 164–171.

Ende, M.T.A., Peppas, N.A., 1997. Transport of ionizable drugs and proteins in crosslinked poly(acrylic acid) and poly(acrylic acid-co-2-hydroxyethyl methacrylate) hydrogels. 2. Diffusion and release studies. J. Contr. Rel. 48, 47–56.

Fristrom, B., 1996. A 6-month, randomized, double-masked comparison of latanoprost with timolol in patients with open angle

glaucoma or ocular hypertension. Acta Opthalmol. Scand. 74, 140–144.

Giambattista, B., Virno, M., Pecori-Giraldi, Pellegrino, N., Motolese, E., 1976. Possibility of isoproterenol therapy with soft contact lenses: ocular hypotension without systemic effects. Ann. Ophthalmol. 8, 819–829.

Graziacascone, M., Zhu, Z., Borselli, F., Lazzeri, L., 2002. Poly(vinyl alcohol) hydrogels as hydrophilic matrices for the release of lipophilic drugs loaded in PLGA nanoparticles. J. Mater. Sci.: Mater. Med. 13, 29–32.

Hehl, E.M., Beck, R., Luthard, K., Guthoff, R., 1999. Improved penetration of aminoglycosides and fluoroquinolones into the aqueous humour of patients by means of Acuvue contact lenses. Eur. J. Clin. Pharmacol. 55, 317–323.

Hillman, J., Masters, J., Broad, A., 1975. Pilocarpine delivery by hydrophilic lens in the management of acute glaucoma. Trans. Ophthal. Soc. U.K., 79–84.

Hillman, J.S., 1974. Management of acute glaucoma with Pilocarpine-soaked hydrophilic lens. Brit. J. Ophthal. 58, 674–679.

Lang, J.C., 1995. Ocular drug delivery conventional ocular formulations. Adv. Drug Delivery 16, 39–43.

Lee, P.J., Sunami, A., Fozzard, H.A., 2001. Cardiac-specific external paths for lidocaine, defined by isoform-specific residues, accelerate recovery from use-dependent block. Circ. Res. 89, 1014–1021.

Mandell, R.B., 1974. Contact Lens Practice: Hard and Flexible Lenses, vol. 3, 2nd ed. Charles C. Thomas, Springfield.

Marmion, V.J., Yardakul, S., 1977. Pilocarpine administration by contact lens. Trans. Ophthal. Soc. U.K. 97, 162–163.

Mc Namara, N.A., Polse, K.A., Brand, R.D., Graham, A.D., Chan, J.S., Mc Kenney, C.D., 1999. Tear mixing under a soft contact lens: effects of lens diameter. Am. J. Ophthal. 127, 659–665.

Merkovich, E.A., Carruette, M.L., Babak, V.G., Vikhoreva, G.A., Gal'braikh, L.S., Kim, V.E., 2001. Kinetics of the initial stage of gelation in chitosan solutions containing glutaric aldehyde: viscometric study. Colloid J. 63, 350–354.

Montague, R., Watkins, R., 1975. Pilocarpine dispensation for the soft hydrophilic contact lens. Brit. J. Ophthal. 59, 455–458.

Nakada, K., Sugiyama, A., 1998. Process for producing controlled drug-release contact lens, and controlled drug-release contact lens thereby produced. United States Patent 6,027,745.

Peppas, N.A., 1987. Hydrogels in Medicine and Pharmacy, vol. 1. CRC Press, Boca Raton, FL.

Podual, K., Doyle, F.J., Peppas, N.A., 2000. Preparation and dynamic response of cationic copolymer hydrogels containing glucose oxidase. Polymer 41, 3975–3983.

Ramer, R., Gasset, A., 1974. Ocular penetration of pilocarpine. Ann. Ophthalmol. 6, 1325–1327.

Rosenwald, P.L., 1981. Ocular device. Patent 4,484,922.

Schultz, C.L., Nunez, I.M., Silor, D.L., Neil, M.L., 1995. Contact lens containing a leachable absorbed material. Patent 5,723,131.

Schultz, C.L., Mint, J.M., 2000. Drug delivery system for antiglaucomatous medication. Patent 6,410,045.

Scott, R.A., Peppas, N.A., 1999. Highly crosslinked, PEG-containing copolymers for sustained solute delivery. Biomaterials 20, 1371–1380.

Segal, M., 1991. Patches, pumps and timed release. FDA Consumer magazine 1991.

Timoptic® prescribing information, supplied by MERCK.

Ward, J.H., Peppas, N.A., 2001. Preparation of controlled release systems by free-radical UV polymerizations in the presence of a drug. J. Contr. Rel. 71, 183–192.

Wilson, M.C., Shields, M.B., 1989. A comparison of clinical variations of the iridocorneal endothelial syndrome. Arch. Ophthalmol. 107, 1465–1468.